# Supporting Information

## Jeong et al. 10.1073/pnas.1715592114

### SI Materials and Methods

**Crystallization and Structure Determination.** For crystallization of zrMmm1, 1 μL of protein solution was mixed with an equal volume of reservoir solution containing 25% (wt/vol) polyethylene glycol (PEG) 10,000 and 100 mM Hepes (pH 7.5), and crystals were grown by hanging drop vapor diffusion at 4 °C. To obtain diffraction-quality single crystals of Se-Met zrMmm1, microseeds of native crystals were added into drops containing a mixture of Se-Met zrMmm1 protein solution and crystallization buffer under the same reservoir conditions. Crystals were cryoprotected by soaking in buffer containing crystallization solution supplemented with 30% (vol/vol) glycerol and flash-frozen in liquid nitrogen. X-ray diffraction data were collected from a single crystal at 100 K at the 5C beamline at the Pohang Accelerator Laboratory with a Pilatus M detector. Data were indexed, integrated, and scaled with the HKL2000 suite (44). Crystals of native and Se-Met zrMmm1 diffracted to 2.8 Å and 3.1 Å resolution, respectively. Crystals grew in space group $P3_221$ with one molecule in the asymmetric unit. The structure of the SMP domain of zrMmm1 was determined by selenium single-wavelength anomalous dispersion at a wavelength of 0.97949. Phenix AutoSol (45) found two selenium sites, refined these to give a mean figure of merit of 0.44, and yielded an initial electron density map of excellent quality. The model of zrMmm1 was refined to $R/R_{free}$ values of 0.194/0.235 via iterative rounds of refinement and rebuilding using Phenix (45) and Coot (46). The final model has good geometry, with 99.6% and 0.4% of residues in favored and generously allowed regions of the Ramachandran plot. The following residues of zrMmm1 were not modeled because of disordered electron density: residues 190–193, residues 357–364, and residues 440–444.

The scMdm12Δ–zrMmm1 complex was crystallized at 18 °C by hanging drop vapor diffusion by mixing 1 μL of the complex with 1 μL of reservoir solution comprising 14% (wt/vol) PEG 4000, 100 mM Hepes (pH 6.5), and 100 mM ammonium sulfate. Because initial crystals diffracted to low resolution (~6.5 Å) using synchrotron radiation, crystals were dehydrated by gradually increasing the percentage of PEG 4000 up to 30%. Crystals were flash-frozen in harvest buffer supplemented with 25% (vol/vol) ethylene glycol. Crystals diffracted to a maximum resolution of 3.8 Å, and diffraction data were processed as previously described. The structure of the scMdm12Δ–zrMmm1 complex was solved by molecular replacement with Phaser-MR (47) using the structures of zrMmm1 (determined in this study) and scMdm12 (Protein Data Bank ID code 5GYD) as search models. The tetramer organized in an scMdm12Δ-zrMmm1-zrMmm1-scMdm12Δ arrangement was found as a molecular replacement solution with a translation-function Z-score of 17.9 in space group $P6_5$. Model building and refinement were completed with Coot (46) and Phenix (45), respectively. The refined model contains residues 194–347, residues 369–390, and residues 395–439 of zrMmm1 as well as and residues 1–73, residues 116–182, and residues 212–265 of Mdm12. All molecular images in figures were generated using PyMOL (https://pymol.org/2/, version 1.7.4.3). Details of crystallographic data and refinement statistics are summarized in Table S1.

**SEC.** To analyze relative molecular weight and assay for interactions between native or truncated scMdm12 and zrMmm1 (Fig. 1*B*), protein samples were prepared in buffer C. Proteins at 1 mg/mL were applied to a Superdex 200 16/60 column (GE Healthcare) at a flow rate of 1 mL/min at 4 °C. In Fig. 6*C*, 300 μg of wild-type proteins (His-zrMmm1 and His-zrMmm1–scMdm12 complex) or mutant proteins [His-zrMmm1 (Y261W) and His-zrMmm1 (Y261W)–scMdm12 complex] were subjected to chromatography on a Superdex 200 10/300 GL (GE Healthcare) column at a flow rate of 0.5 mL/min at 4 °C. A GE Healthcare gel-filtration calibration kit was used with protein standards (ferritin, 440 kDa; aldolase, 158 kDa; conalbumin, 75 kDa; ovalbumin, 44 kDa; carbonic anhydrase, 29 kDa; and ribonuclease A, 13.7 kDa).

**Pull-Down Assay.** For GST pull-down, wild-type zrMmm1 and mutants zrMmm1 (L315S and L327S) were cloned into the pGEX-6p1 vector, and scMdm12 (wild-type, L56S, I59S, I119S, and F121S) was cloned into the pCDF-duet vector using NdeI and XhoI. Supernatants from *Escherichia coli* coexpressing wild-type or mutant scMdm12 and zrMmm1 were incubated with 10 μL of glutathione Sepharose 4B beads (GE Healthcare) preequilibrated with buffer A at 4 °C for 1 h. Beads were washed three times with buffer A containing 0.5% (vol/vol) Nonidet P-40 and 0.1% (vol/vol) Triton X-100. Proteins were eluted with 4× SDS sample buffer, and analyzed by SDS/PAGE and Coomassie Blue staining.

**In Vitro Lipid Displacement Experiments.** For the lipid displacement experiments shown in Figs. 3*D* and 6*A*, the N-terminal His-tagged zrMmm1 (His-zrMmm1) or His-zrMmm1–scMdm12 complex was incubated with a twofold molar excess of NBD-PE purchased from Avanti Polar Lipids overnight on ice in buffer D (buffer C containing 0.3 mM *N*,*N*-dimethyldodecylamine *N*-oxide; Sigma–Aldrich). To remove excess unbound NBD-PE, the mixture was incubated with Ni-nitrilotriacetic acid agarose beads (QIAGEN) for 30 min, and washed three times with buffer D. NBD-PE bound to His-zrMmm1 or His-zrMmm1–scMdm12 complex was eluted with buffer D containing 200 mM imidazole, and the protein solution was dialyzed against buffer D overnight and concentrated to 1 mg/mL. His-zrMmm1 or His-zrMmm1–scMdm12 complex (8 μL) preloaded with NBD-PE was mixed with 11 μL of buffer D and 1 μL of phospholipids dissolved in methanol. Reaction mixtures were further incubated for 2 h on ice, and analyzed by native PAGE as described previously (20). Lipid displacement experiments involving mutants, His-zrMmm1 (Y261W) or His-zrMmm1 (Y261W)–scMdm12 complex, were performed in the same way as described above. All phospholipids were purchased from Avanti Polar Lipids: PA (1,2-dioleoyl-*sn*-glycero-3-phosphate), PC (1,2-dioleoyl-*sn*-glycero-3-phosphocholine), PE (1,2-dioleoyl-*sn*-glycero-3-phosphoethanolamine), PG (1,2-dioleoyl-*sn*-glycero-3-phospho-[1′-rac-glycerol]), and PS (1,2-dioleoyl-*sn*-glycero-3-phospho-L-serine). Nonphospholipid ligands, cholesterol (Sigma–Aldrich), ergosterol (Tokyo Chemical Industry), and ceramide (*N*-oleoyl-D-erythro-sphingosine; C18:1 Ceramide [d18:1/18:1(9Z)]; Avanti Polar Lipids) were used.

**Lipid-Binding Assays.** For the lipid-binding assays shown in Fig. 3*E*, 19 μL of 0.5 mg/mL His-zrMmm1 (wild-type or mutants) in buffer D was mixed with 1 μL of 1 mg/mL 18:1 NBD-PE on ice. After 2 h, reaction products were subjected to 12% blue native (BN)-PAGE and analyzed as described above. BN-PAGE was carried out using the method of Schägger and von Jagow (48).

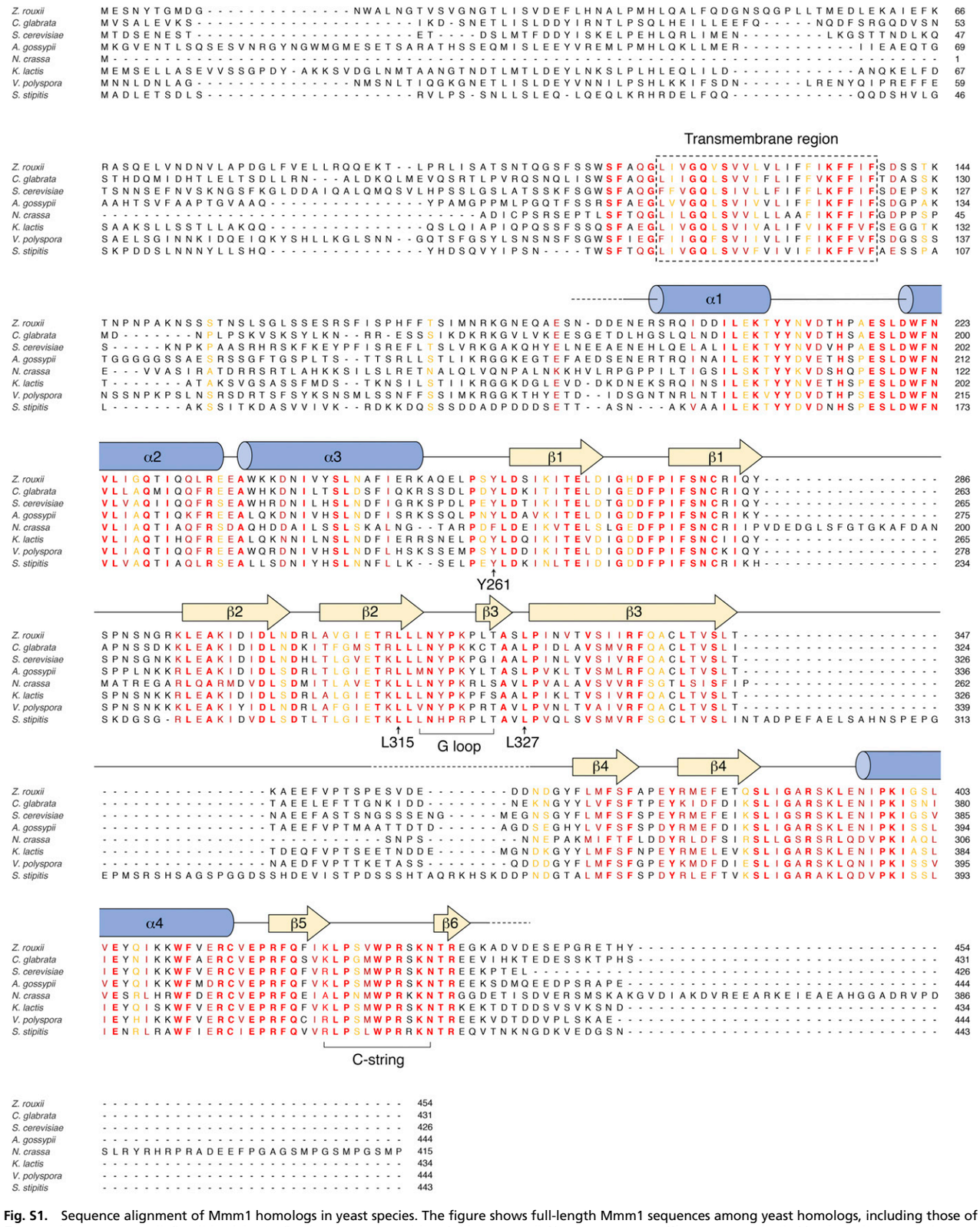


**Fig. S1.** Sequence alignment of Mmm1 homologs in yeast species. The figure shows full-length Mmm1 sequences among yeast homologs, including those of *Zygosaccharomyces rouxii*, *Candida glabrata*, *Saccharomyces cerevisiae*, *Ashbya gossypii*, *Neurospora crassa*, *Kluyveromyces lactis*, *Vanderwaltozyma polyspora*, and *Scheffersomyces stipitis*. The sequence conservation at each amino acid is shaded in a color gradient from yellow (70% similarity) to red (100% identity). The secondary structure assigned by the crystal structure of zrMmm1 (residues 190–444) is indicated above the sequences as blue cylinders (α-helices), yellow arrows (β-strands), black lines (loop regions), and black dots (disordered residues). Putative transmembrane domains required for anchoring the ER membrane are highlighted with a dotted box. Two conserved and significant residues (L315 and L327) involved in the interaction with Mdm12 are indicated below the sequences.

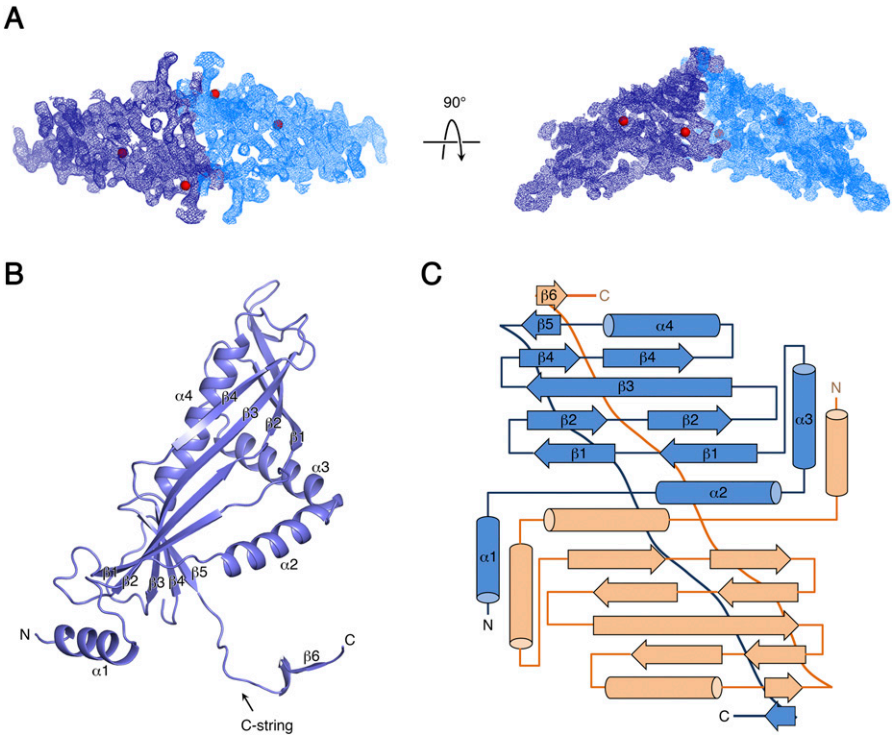


**Fig. S2.** Structural analysis of the zrMmm1 SMP domain. (*A*) Experimental electron density map (contoured at the 1.0 σ level at 3.1 Å resolution) for zrMmm1 in the dimeric SMP configuration. Crystals of zrMmm1 have one molecule of zrMmm1 in the asymmetric unit. Two protomers of zrMmm1 are organized by crystallographic symmetry in the $P3_221$ space group. The map was calculated using single-wavelength anomalous diffraction phases after density modification. Red spheres represent selenium atoms found by the Phenix program (45). (*B*) Overall structure of the SMP domain of zrMmm1, showing the four α-helices and six β-strands. (*C*) Schematic diagram showing the secondary structure elements and their organization in the zrMmm1 dimer.

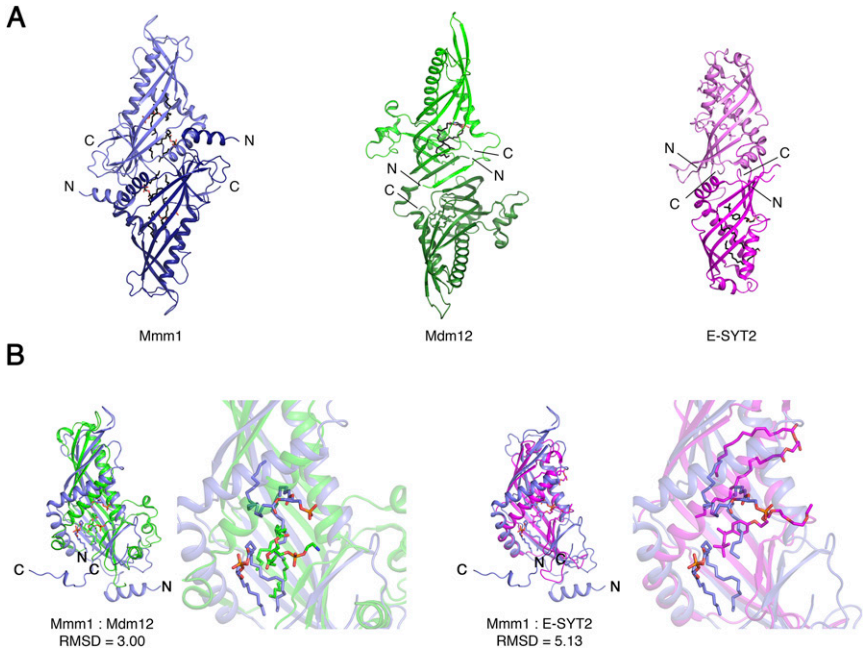


**Fig. S3.** Structural comparison of the SMP domains of zrMmm1, Mdm12, and E-SYT2. (*A*) Ribbon diagrams showing the overall structure of the SMP domain of zrMmm1, Mdm12 [Protein Data Bank (PDB) ID code 5GYD], and E-SYT2 (PDB ID code 4P42) in the same orientation. The zrMmm1, E-SYT2, and Mdm12 are colored blue, red, and green, respectively. (*B*) Structural comparison of the zrMmm1 SMP domain (blue) aligned with those of *S. cerevisiae* Mdm12 (green, rmsd of 3.0 Å) and *Homo sapiens* E-SYT2 (red, rmsd of 5.13 Å). Phospholipid molecules bound to each protein are shown in ball-and-stick representation.

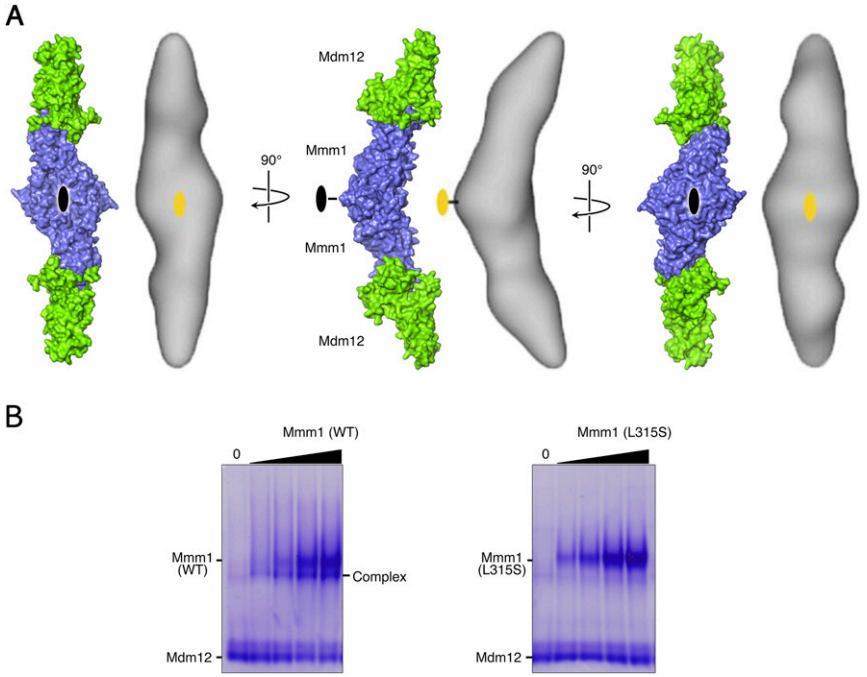


**Fig. S4.** Structural alignment of the crystal structure and EM structure of the Mdm12–Mmm1 complex. (*A*) Comparison of the 3.8 Å crystal structure of the scMdm12–zrMmm1 complex determined in this study and the 17 Å resolution negative-staining EM map of the Mdm12–Mmm1 complex presented previously (19). Both structures revealed that the SMP domains of the Mmm1 dimer are located at the center and capped by two Mdm12 molecules, one at each end. The zrMmm1 and scMdm12 are colored blue and green, respectively. Twofold symmetry axes are indicated with yellow and black circles. For complete comparison, the structure of scMdm12Δ in the scMdm12Δ–zrMmm1 complex was replaced with that of the full-length scMdm12 (PDB ID code 5GYD) in this figure. (*B*) Purified zrMmm1 [wild-type (WT) and L315S mutant] proteins were incubated with purified scMdm12 at different concentrations, and mixtures were separated by 8% native PAGE and stained with Coomassie Blue.

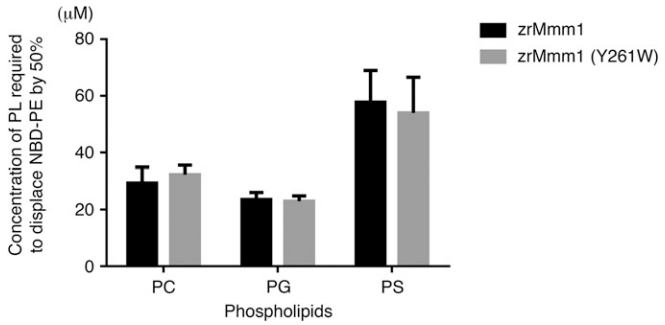


**Fig. S5.** In vitro phospholipid displacement of wild-type and mutant (Y261W) zrMmm1. To confirm Y261W mutant did not affect lipid-binding properties of zrMmm1 alone, in vitro phospholipid displacement experiments were performed using wild-type zrMmm1 and the Y261W mutant of zrMmm1. The graph indicates the concentration of phospholipid (PC, PG, and PS) that reduced NBD-PE fluorescence by 50%. The bar graph shows means ± SD ($n = 3$).

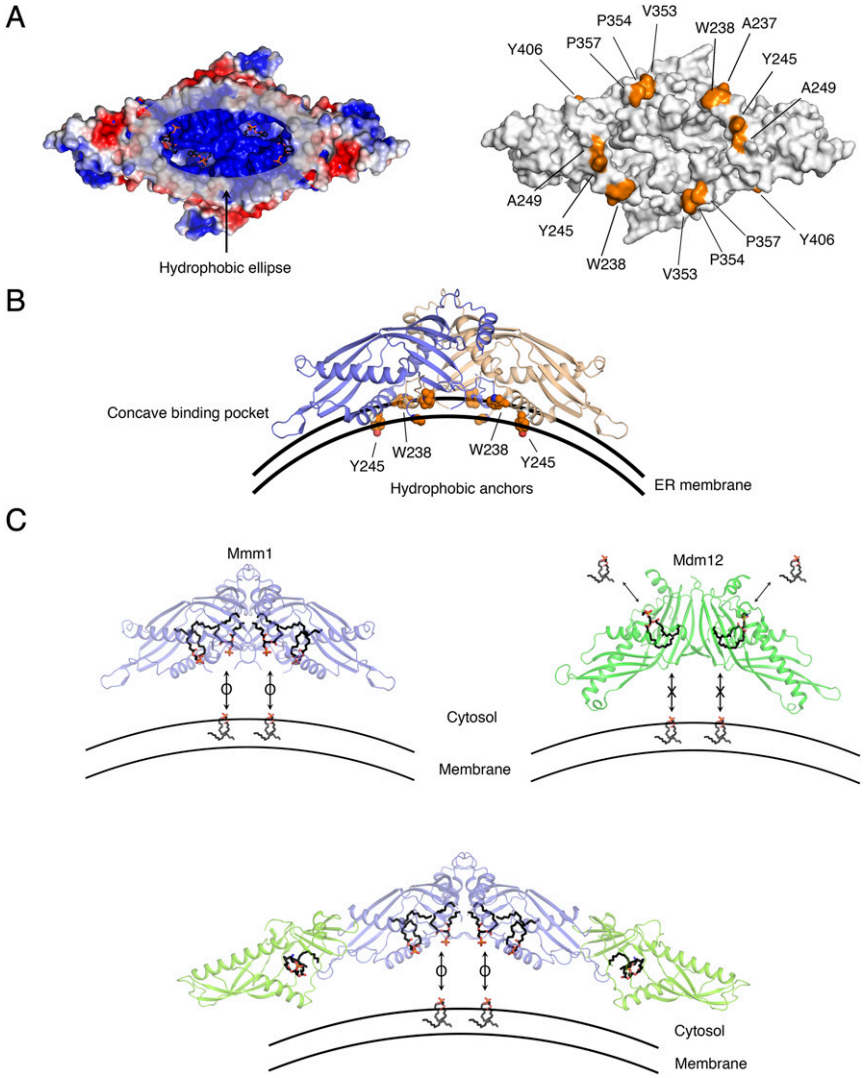


**Fig. S6.** Concave surface of the Mmm1 SMP domain apposes the ER membrane. (*A*, *Left*) Surface charge representation of zrMmm1 viewed from the concave surface. (*A*, *Right*) Positively charged patch in the center is surrounded by conserved hydrophobic residues (yellow) that might be involved in anchoring to the ER membrane. (*B*) Diagram showing the overall structure of the zrMmm1 dimer. This view is rotated 90° about the horizontal axis relative to *A*. Black lines indicate the putative curvature of the ER membrane. Side chains of the hydrophobic residues indicated in *A* are shown in surface-filling representation. (*C*, *Top*) Ribbon diagrams show the arch-shaped dimeric SMP structure of the zrMmm1 (*Left*) and scMdm12 (*Right*, PDB ID code 5GYD). The view is the same as in *B*. The figures highlight the positions of phospholipids bound to zrMmm1 or scMdm12. Head groups of phospholipids bound to zrMmm1 face the ER membrane, whereas those bound to scMdm12 project toward the opposite side of the ER membrane, suggesting that zrMmm1 might take phospholipids from the ER. (*C*, *Bottom*) Concave surface shown in the scMdm12–zrMmm1 complex corresponds to the concave inner surface of zrMmm1 alone.

**Table S1. Data collection and refinement statistics**

| | zrMmm1 | | scMdm12Δ–zrMmm1 |
|---|---|---|---|
| | Native dataset | Se SAD dataset | Native dataset |
| PDB ID code | 5YK6 | | 5YK7 |
| X-ray source | Beamline 5C, PAL | Beamline 5C, PAL | Beamline 5C, PAL |
| Temperature, K | 100 | 100 | 100 |
| Space group | $P3_221$ | $P3_221$ | $P6_5$ |
| Cell dimensions | | | |
| a, b, c; Å | 125.50, 125.50, 60.88 | 125.60, 125.60, 60.90 | 87.56, 87.56, 436.88 |
| α, β, γ; ° | 90.00, 90.00, 120.00 | 90.00, 90.00, 120.00 | 90.00, 90.00, 120.00 |
| Data processing | | | |
| Wavelength, Å | 0.97949 | 0.97950 | 0.97950 |
| Resolution, Å | 50.0–2.80 (2.85–2.80) | 50.0–3.10 (3.15–3.10) | 50.0–3.80 (3.87–3.80) |
| $R_{merge}$, % | 7.4 (39.5) | 8.5 (39.0) | 4.6 (83.6) |
| CC1/2 | 0.999 (0.354) | 0.999 (0.847) | 0.999 (0.741) |
| I/σI | 26.8 (1.81) | 16.6 (2.09) | 27.5 (1.43) |
| Completeness, % | 99.2 (98.5) | 99.3 (97.3) | 99.8 (99.4) |
| Redundancy | 9.4 (4.8) | 6.7 (4.7) | 5.8 (4.9) |
| Measured reflections | 130,987 | 130,066 | 107,706 |
| Unique reflections | 13,895 | 19,357 | 18,583 |
| Refinement statistics | | | |
| Data range, Å | 41.1–2.80 | | 39.14–3.80 |
| Reflections | 13,887 | | 18,456 |
| R-factor, % | 19.36 | | 23.76 |
| $R_{free}$, % | 23.49 | | 26.24 |
| No. of nonhydrogen atoms | 2,059 | | 6,817 |
| rmsds | | | |
| Bond lengths, Å | 0.008 | | 0.003 |
| Bond angles, ° | 1.387 | | 0.772 |
| Ramachandran plot, residues in | | | |
| Most favored, % | 92.4 | | 84.6 |
| Additional allowed, % | 7.2 | | 14.9 |
| Generously allowed, % | 0.4 | | 0.5 |
| Disallowed, % | 0 | | 0 |

Values in parentheses are for the respective highest-resolution shells. PAL, Pohang Accelerator Laboratory; SAD, single-wavelength anomalous dispersion.